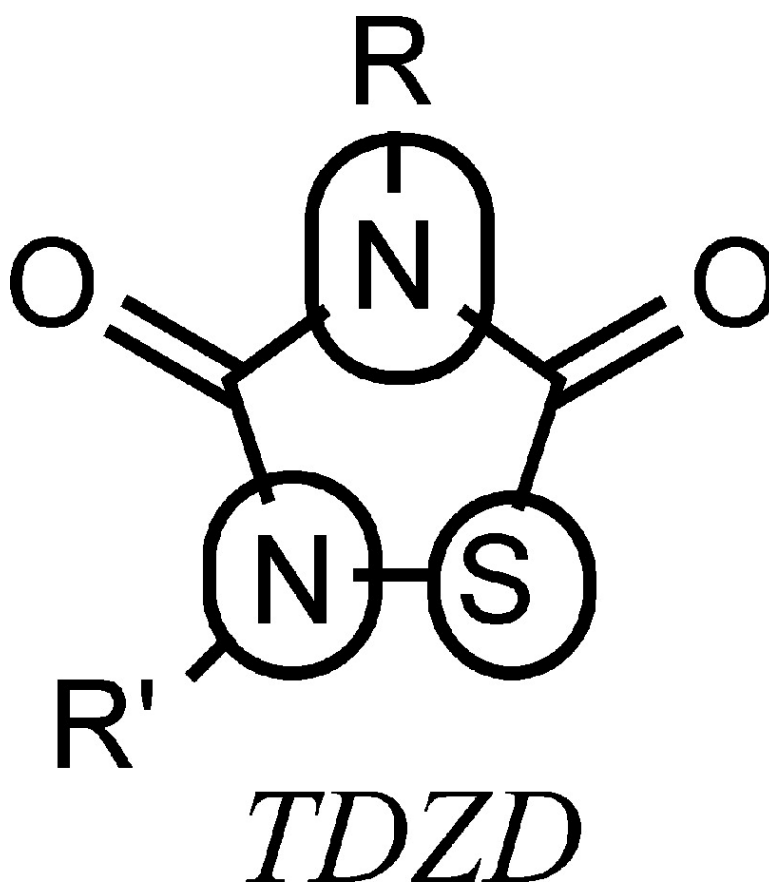


SAR and 3D-QSAR Studies on Thiadiazolidinone Derivatives: Exploration of Structural Requirements for Glycogen Synthase Kinase 3 Inhibitors

Ana Martinez, Mercedes Alonso, Ana Castro, Isabel Dorronsoro, J. Luis Gelp, F. Javier Luque, Concepcin Prez, and Francisco J. Moreno

J. Med. Chem., **2005**, 48 (23), 7103-7112 • DOI: 10.1021/jm040895g • Publication Date (Web): 08 October 2005

Downloaded from <http://pubs.acs.org> on March 29, 2009



More About This Article

Additional resources and features associated with this article are available within the HTML version:

- Supporting Information



Journal of Medicinal Chemistry

Subscriber access provided by American Chemical Society

- Links to the 6 articles that cite this article, as of the time of this article download
- Access to high resolution figures
- Links to articles and content related to this article
- Copyright permission to reproduce figures and/or text from this article

[View the Full Text HTML](#)



ACS Publications
High quality. High impact.

Journal of Medicinal Chemistry is published by the American Chemical Society, 1155
Sixteenth Street N.W., Washington, DC 20036

Articles

SAR and 3D-QSAR Studies on Thiadiazolidinone Derivatives: Exploration of Structural Requirements for Glycogen Synthase Kinase 3 Inhibitors

Ana Martínez,^{*,†,‡} Mercedes Alonso,^{†,‡} Ana Castro,^{†,‡} Isabel Dorronsoro,^{†,‡} J. Luis Gelpí,[§] F. Javier Luque,^{||} Concepción Pérez,[†] and Francisco J. Moreno[‡]

Instituto de Química Médica (CSIC), Juan de la Cierva 3, 28006 Madrid (Spain), Centro de Biología Molecular “Severo Ochoa” (CSIC-UAM), Universidad Autónoma de Madrid, 28049 Madrid (Spain), Departamento de Bioquímica y Biología Molecular Facultad de Química, Universidad de Barcelona, Martí i Franqués 1, 08028 Barcelona (Spain), and Departamento de Fisicoquímica, Facultad de Farmacia, Universidad de Barcelona, Av. Diagonal 643, 08028 Barcelona (Spain)

Received November 16, 2004

The 2,4-disubstituted thiadiazolidinones (TDZD) are described as the first ATP-noncompetitive GSK-3 inhibitors. Following an SAR study about TDZD, different structural modifications in the heterocyclic ring aimed to test the influence of each heteroatom on the biological study are here reported here. Various compounds such as hydantoin, dithiazolidinones, rhodanines, maleimides, and triazoles were synthesized and screened as GSK-3 inhibitors. After an extensive SAR study among these different heterocyclic families, TDZDs have been revealed as a privileged scaffold for the selective inhibition of GSK-3. A CoMFA analysis was also performed highlighting the molecular electrostatic field interaction in the interaction of TDZDs with GSK-3. Moreover, first mapping studies indicate two binding modes which in turn might imply relevant differences in the mechanism that underly the inhibitory activity of TDZDs.

Introduction

Glycogen synthase kinase-3 (GSK-3) is a ubiquitous serine/threonine kinase which plays a key role in a large number of cellular processes and diseases. Two functional aspects make GSK-3 a peculiar kinase: its activity is constitutive and down regulated after cell activation by phosphorylation or interaction with inhibitory proteins, and the enzyme prefers substrates that are prephosphorylated by other kinases.¹ Its pleiotropic but unique activities have made GSK-3 a much sought-after target for the treatment of prevalent human diseases² such as type 2 diabetes,³ Alzheimer's disease,⁴ CNS disorders such as manic depressive disorder and neurodegenerative diseases, and chronic inflammatory disorders.⁵

Nowadays, the search for GSK-3 inhibitors is a very active research field for both academic centers and pharmaceutical companies.^{6,7} The most frequent approach until now for discovering GSK-3 inhibitors has exploited screening programs, specifically aimed at finding new ‘hits’ which exhibit other pharmacological profiles. This is the case for kinase inhibitors hymenialdisine,⁸ paullones,⁹ indirubins,¹⁰ maleimides,¹¹ and TDZDs¹² (Figure 1). However, because of the availability of X-ray crystallographic data of GSK-

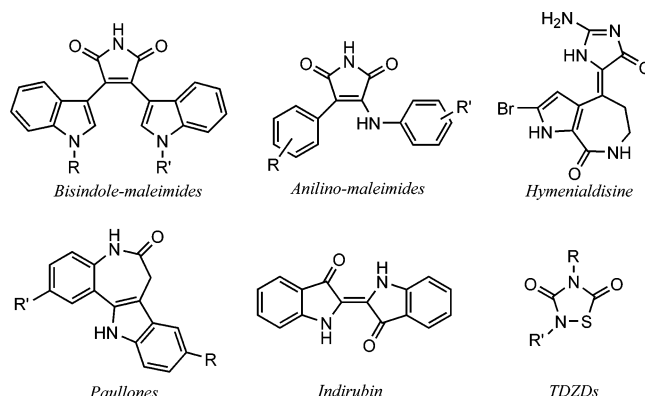


Figure 1. Common GSK-3 inhibitors.

3 β ,^{13–17} rational drug optimization is now being applied to discover new lead compounds.¹⁸

Among the great diversity of chemical structures with GSK-3 inhibition already found,¹⁹ the 2,4-disubstituted thiadiazolidinones (TDZD) are presented as the first ATP-noncompetitive GSK-3 inhibitors.¹² These compounds are of great interest since they did not show inhibitory activity on other kinases such as PKA, PKC, CK-2, and CDK1/cyclin B. Preliminary structure–activity relationship (SAR) studies suggested that the substituent attached to the N2 of the thiadiazolidinone ring, as well as the nature of the substituent of N4, seems to be important for GSK-3 inhibition. Moreover, both C5 and C3 carbonyl groups could mediate favorable interactions with the enzyme.

In this study different structural modifications are introduced in the heterocyclic ring with the aim to test the influence of each heteroatom on the biological

* Corresponding author. Tel 91-8061130 Fax: 91-8034660, e-mail: amartinez@neuropharma.es.

[†] Instituto de Química Médica (CSIC).

[‡] Universidad Autónoma de Madrid.

[§] Departamento de Bioquímica y Biología Molecular Facultad de Química, Universidad de Barcelona.

^{||} Departamento de Fisicoquímica, Universidad de Barcelona.

[‡] Present address: NeuroPharma, S.A.; Avda. de la Industria 52, 28760 Tres Cantos, Madrid (Spain).

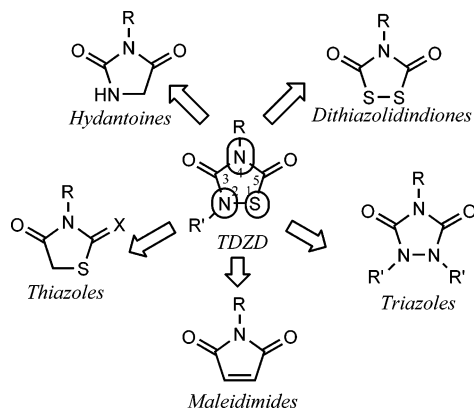
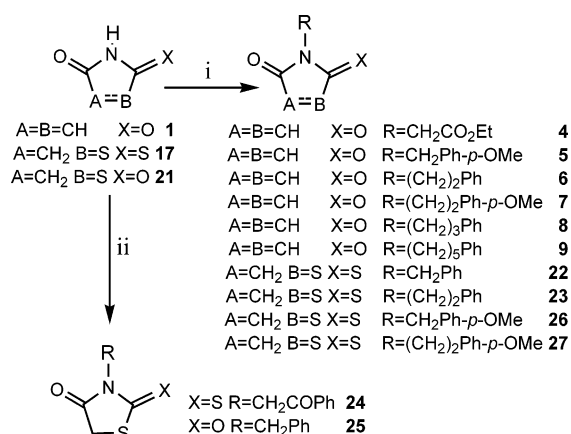


Figure 2. Schematic representation of the structural differences in the heteroaromatic rings of the different classes of compounds considered in the study.

Scheme 1^a



^a Reagents: (i) R-OH, Ph₃P, DIAD or DEAD, THF, rt, 24 h; (ii) R-X, alkaline medium, CH₃COCH₃.

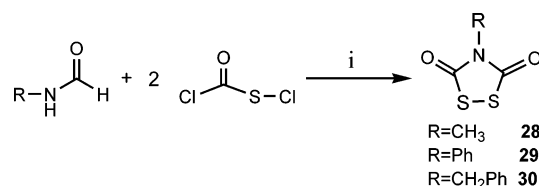
activity. Thus, the biological activity of a large set of different heterocyclic compounds structurally related to TDZDs was evaluated. The common scaffold was a pentagonal ring containing carbonyl and thiocarbonyl groups in a 1,3 relative disubstitution. Among these heterocycles we have screened as GSK-3 inhibitors different compounds such as hydantoins, dithiazolidindiones, rhodanines, maleimides, and triazoles (Figure 2). The CoMFA methodology,²⁰ in conjunction with mapping studies, are used to gain insight into the molecular determinants that mediate the GSK-3 inhibitory activity of these compounds.

Chemistry. The chemical modifications on the different target heterocyclic systems, except for dithiazolidinedione, were achieved using the more suitable method of alkylation in each case. Thus, maleimides 4–9 and some rhodanine derivatives (compounds 22, 23, 26, and 27) were prepared using Mitsunobu reaction modification,²¹ whereas N-alkylation of the rhodanine ring to yield 24 and 25 derivatives occurred using a weak base and the corresponding alkyl halide in acetone (Scheme 1).

A previously described method²² using chlorocarbonylsulfonyl chloride with different formamides was selected for the preparation of dithiazolidinedione derivatives 28–30 (Scheme 2).

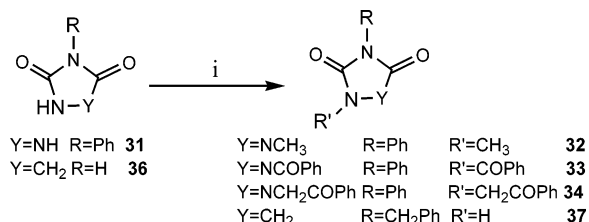
Different triazolidinedione (compounds 32–34) and hydantoin (compound 37) derivatives were synthesized

Scheme 2^a



^a Reagents: (i) THF or toluene, r.t., 20 h.

Scheme 3^a



^a Reagents: (i) R'-X (X = Cl, Br, I), alkaline medium.


using the commercial 4-phenyl-urazole (compound 31) or hydantoin (compound 36), respectively, as starting material under classical alkylation conditions (alkaline medium and alkyl halide)²³ (Scheme 3).

Biological Results and SAR Studies. Maleimides. The maleimide derivatives are an important family of compounds in chemical²⁴ and biochemical areas.^{25,26} The maleimide scaffold could be considered structurally related to the TDZD, one in which two heteroatoms, the sulfur atom, and the nitrogen directly attached to it are eliminated. However, the planarity of the ring is preserved with the double bond between both carbon atoms.

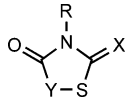
Our previous study on TDZDs¹² indicated that the attachment of aromatic or hydrophobic substituents at N4 leads to an increase of the activity. Therefore, derivatives where the nitrogen atom is bonded through different linkers to an aromatic ring containing functional groups capable of establishing hydrogen-bond interactions or an ester group were prepared. These new derivatives (compounds 4–9), together with a wide set of commercially available related compounds (compounds 1–3 and 10–16), were evaluated as GSK-3 inhibitors following the method described in the Experimental Section.

In general, these compounds are GSK-3 inhibitors at micromolar level (see Table 1). Inhibitory activity increased when the nitrogen atom of the maleimide ring was substituted by any aromatic or ester substituent (compound 1 and 2 versus 3–5). Moreover, the length of the linker between the aryl group and the heterocyclic nitrogen does not influence the inhibitory activity (compounds 6–9). Considering the nature of the atom that bridges the two carbonyl groups, the inhibitory activity decreases in the sequence N>C ≫ O (compounds 1, 10, and 11). Finally, it is clear that the presence of carbonyl groups and the double bond between the two carbons attached to the carbonyl groups are prerequisites for the inhibitory activity (compounds 13–16).

Rhodanines and Thiazolidines. These compounds, which have a broad pharmacological profile (antibacterial,²⁷ antiviral,²⁸ anticonvulsive,²⁹ and antihyperglycemic³⁰ activity), differ from TDZDs by the presence of only one nitrogen atom in the ring. Even though some

Table 1. GSK-3 Inhibition of Maleimide-Related Compounds


compd	X	Y	Z	A	B	R	IC ₅₀ (μM)
1	CH	CH	N	C=O	C=O	H	6
2	CH	CH	N	C=O	C=O	CH ₃	5
3	CH	CH	N	C=O	C=O	CH ₂ Ph	1
4	CH	CH	N	C=O	C=O	CH ₂ CO ₂ Et	3
5	CH	CH	N	C=O	C=O	CH ₂ Ph-p-OCH ₃	2.5
6	CH	CH	N	C=O	C=O	(CH ₂) ₂ Ph	2
7	CH	CH	N	C=O	C=O	(CH ₂) ₂ Ph-p-OCH ₃	3
8	CH	CH	N	C=O	C=O	(CH ₂) ₃ Ph	3
9	CH	CH	N	C=O	C=O	(CH ₂) ₅ Ph	3
10	CH	CH	CH ₂	C=O	C=O		12
11	CH	CH	O	C=O	C=O		> 100
12	CH ₂	CH ₂	CH ₂	C=O	C=O		> 100
13	CH ₂	CH ₂	N	C=O	C=O	H	> 100
14	CH ₂	CH ₂	N	C=O	C=O	CH ₂ Ph	> 50
15	CH ₂	CH ₂	N	C=O	CH ₂	CH ₂ Ph	> 100
16	CH	CH	N	CH ₂	CH ₂	CH ₂ Ph	> 100

Table 2. GSK-3 Inhibition of the Rhodanine-Related Derivatives


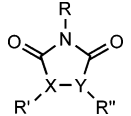
compd	X	Y	R	IC ₅₀ (μM)
17	S	CH ₂	H	100
18	S	CH ₂	CH ₃	100
19	S	CH ₂	CH ₂ COOH	100
20	S	CH ₂	NH ₂	100
21	O	CH ₂	H	100
22	S	CH ₂	Bn	25
23	S	CH ₂	(CH ₂) ₂ Ph	35
24	S	CH ₂	CH ₂ COPh	50
25	O	CH ₂	Bn	100
26	S	CH ₂	Bn-p-OMe	65
27	S	CH ₂	(CH ₂) ₂ Ph-p-OMe	100

of them are commercially available (compounds **17–21**), we introduced different aromatic or hydrogen-bonding acceptor substituents at the nitrogen position in order to increase the chemical diversity among these structures (compounds **22–27**).

The GSK-3 inhibition data are given in Table 2. The *N*-benzyl-rhodanine derivative (compound **22**) was found to have the best inhibitory activity, thus supporting the important role played by the aromatic substituent at this position. However, the activity diminishes when the linker between the aromatic moiety and the nitrogen atom is longer (compound **23**). More remarkably, the presence of a thiocarbonyl group is a prerequisite for activity in these compounds, as its replacement by a carbonyl group (compare compound **22**–compound **25**) is detrimental.

Dithiazolidinediones, Triazolinediones, and Hydantoins. 1,2,4-Dithiazolidine-3,5-diones derivatives bear a sulfur atom instead of the nitrogen atom at position 2 in TDZDs. In contrast, in triazolinedione ring a nitrogen atom replaces the sulfur atom present in TDZDs. Finally, some hydantoin compounds, where the sulfur atom is replaced by carbon, were also included in the study.

The results of the biological assays against GSK-3 (Table 3) corroborated our previous findings. Thus, an

Table 3. GSK-3 Inhibition of Dithiazolidinedione, Triazolinedione, and Hydantoin Derivatives


compd	X	Y	R	R'	R''	IC ₅₀ (μM)
28	S	S	CH ₃	–	–	100
29	S	S	Ph	–	–	12
30	S	S	CH ₂ Ph	–	–	12
31	N	N	Ph	H	H	100
32	N	N	Ph	CH ₃	CH ₃	100
33	N	N	Ph	COPh	COPh	100
34	N	N	Ph	CH ₂ COPh	CH ₂ COPh	100
35	N	N	Ph	–	–	100
36	N	CH ₂	H	H	–	100
37	N	CH ₂	CH ₂ Ph	H	–	100

aromatic substituent attached to the nitrogen atom, flanked by the two carbonyl groups, seems to be important for activity (compound **28** versus **29** and **30**). However, the activity, nevertheless, is completely lost in triazolinedione and hydantoin compounds, which suggests a crucial role for the sulfur atom of the TDZD scaffold in modulating the inhibitory activity against GSK-3.

Mode of Inhibition and Selectivity Studies. To verify the ATP noncompetitive mechanism of action and the selectivity of TDZD compounds and the rest of derivatives examined in this study, several kinetic and selectivity experiments were performed. Kinetic analysis were carried out using combinations of six ATP concentrations (from 6.5 to 100 μM) and two inhibitor concentrations for two different GSK-3 inhibitors: a derivative of dithiazolidinedione family (compound **30**) and a compound of the known TDZD family (compound **44**). Figure 3 shows that while the enzyme maximal rate decreases in the presence of the inhibitor, the Michaelis constant remains unaltered, thus indicating that compounds **30** and **44** act as ATP-non competitive inhibitors.

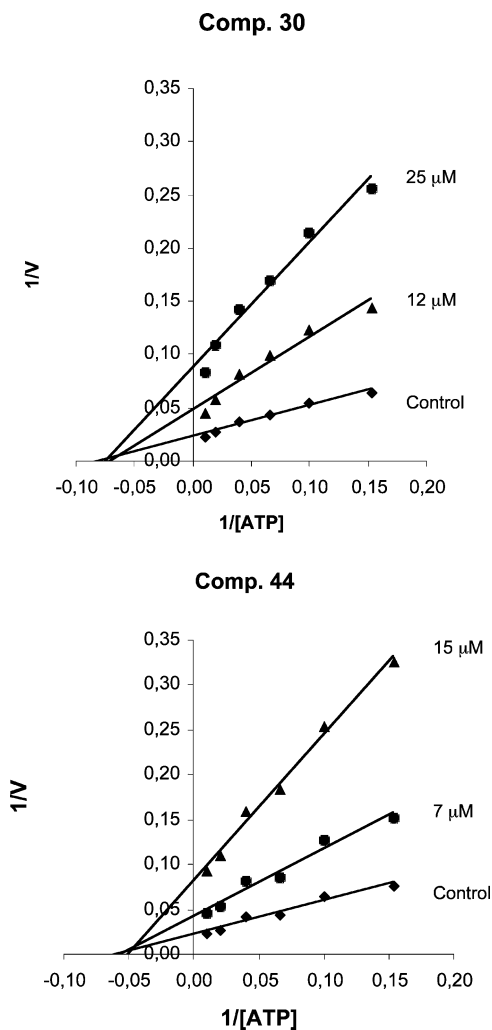
Selectivity of kinase inhibition is critical for pathway analysis in vivo and in cellular systems. In our previous studies¹² TDZD compounds did not show inhibitory activity on PKA, PKC, CK-2, and CDK1/cyclin B. To further examine the selectivity profile of the TDZD family, some of the more representative TDZD compounds (**41**, **43**, **45**, **50**, **55**, and **59**) were evaluated against a panel of seven related kinases: Abl-K, CAM KII, EGF-TyrK, IRK MAPK, MEK1K, and PKp56. The inhibitory assays were performed by using a 10 μM concentration for the different inhibitors. The results reported in Table 4 show that TDZD compounds do not in general have a significant inhibitory effect on the whole set of kinases, which in turn demonstrates the remarkable specificity of TDZD with respect to GSK-3.

CoMFA and Mapping Studies. The preceding data pointed out the important role played by the nature of the heteroaromatic ring and by certain substituents in mediating the GSK-3 inhibition. To further explore the relationship between the chemical structure and the biological activity of TDZDs, a 3D-QSAR study was carried out by using CoMFA methodology. For this purpose, we selected 48 compounds, which include a variety of TDZDs (compounds **38–57**; Table 5) as well as representative members of the other heterocyclic

Table 4. Inhibitory Activity (% inhibition)^a Exhibited by Selected TDZD Compounds for Several Kinases

compd (10 μ M)	Abl-K	CAM K II	EGF-TyrK	IRK	MAP K	MEK 1 K	PK p 56
41	–	23	–	–	–	–	–
43	–	16	25	20	–	–	35
45	–	35	–	19	–	–	27
50	–	–	17	36	–	–	–
55	–	–	40	46	10	–	–
59	–	15	19	50	–	19	–

^a The symbol – indicates an inhibition of less than 10%.

**Figure 3.** Double-reciprocal plot of kinetic data determined for compounds **30** and **44**. Each point is the mean of two different experiments, each one analyzed in duplicate.

compounds examined here (compounds **1–19**, **22–25**, **28**, **31**, **32**, and **35**).

CoMFA models were calculated for each molecular field considered alone or in combination (see Table 6). The best PLS analysis was obtained by combining steric and electrostatic fields (see model D in Table 6), leading to a good correlation between the IC₅₀ values predicted from the principal components extracted from these two fields and the experimental data ($r^2 = 0.922$, $q^2 = 0.654$, and $n = 5$; see Figure 4). To further validate model D, we have attempted to predict the activities of five representative compounds not included in the training set (compounds **4**, **5**, **7**, **58**, and **59**). The predicted IC₅₀ values are also in good agreement with experimental values, which gives support to the predictive power of the model.

Table 5. GSK-3 Inhibition of TDZD Compounds **38–59** Used in the CoMFA Study

compd	R	R'	IC ₅₀ (μ M)
38	Et	Me	5
39	Et	Pr	10
40	Et	<i>i</i> Pr	35
41	Et	c-hex	10
42	Et	Et	25
43	Bn	Me	2
44	Bn	Et	7
45	Bn	Bn	10
46	Ph	Me	2
47	Ph- <i>p</i> -Br	Me	1.1
48	Ph- <i>m</i> -Br	Me	4
49	Ph- <i>o</i> -Br	Me	6
50	Ph- <i>p</i> -CF ₃	Me	6
51	Ph- <i>p</i> -Cl	Me	4
52	Ph- <i>p</i> -F	Me	4
53	Ph- <i>p</i> -OMe	Me	2
54	Ph- <i>p</i> -Me	Me	5
55	Ph- <i>p</i> -NO ₂	Et	8.5
56	1-naphthyl	Me	2
57	c-hex	Me	100
58	Ph	Et	6
59	CH ₂ CO ₂ Et	Me	2

Table 6. Statistical Results^a of CoMFA Analysis

model	field	q^2	n	r^2	s	F
A	steric	0.403	5	0.862	0.251	49.85
B	electrostatic	0.495	3	0.775	0.313	48.22
C	h bond	0.194	2	0.393	0.507	13.92
D	steric+electrostatic	0.654	5	0.922	0.189	94.32
E	steric+lipophilic	0.274	2	0.498	0.462	21.30
F	electrostatic+ lipophilic	0.440	4	0.780	0.313	36.33
G	steric+electrostatic + lipophilic	0.556	5	0.859	0.253	48.84

^a q^2 , n , r^2 , s , and F are the squared cross-validated correlation coefficient, the number of components, the squared correlation coefficient, the standard deviation of regression equation, and the F ratio, respectively.

Table 7. IC₅₀ Data (μ M) for GSK-3 Inhibitors Including in the CoMFA Validation Set

compound	experimental	predicted
4	3	3.8
5	2.5	3.5
7	3	3
58	6	17
59	2	3.5

Since the relative contributions of steric and electrostatic molecular field were 42% and 58%, respectively, it seems that the inhibitory activity in TDZD and related compounds is modulated by a subtle balance of the two fields. Figure 5 shows the graphical representation of CoMFA results. Sterically favorable regions

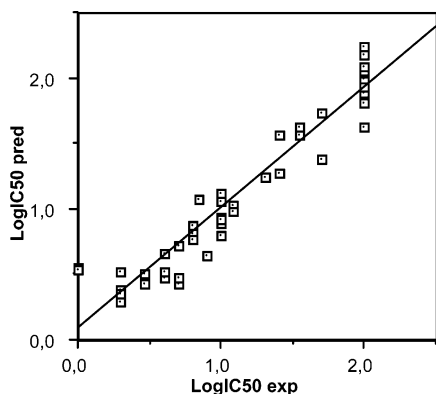


Figure 4. Graphical representation of experimental and predicted (model D) IC_{50} data for compounds included in the training set.

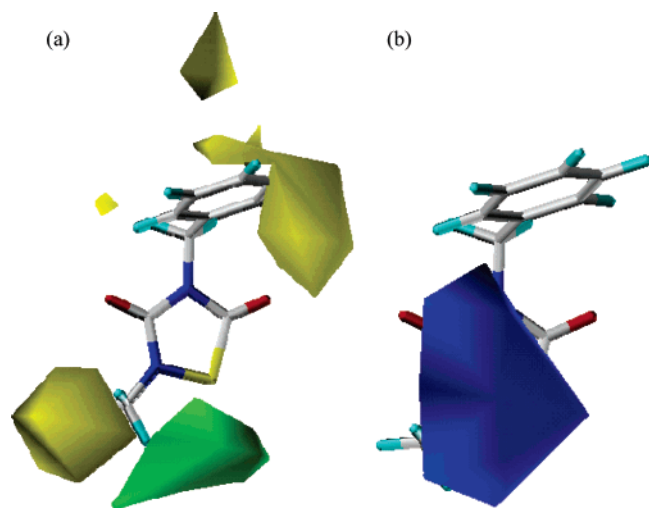


Figure 5. Graphical representation of CoMFA analysis (model D). (a) Steric contour plots: The yellow area represents the region where an increase of steric bulk is predicted to increase activity, whereas the green area represents the region where an increase of steric bulk is predicted to decrease activity. (b) Electrostatic contour plots: blue contour means the region where a negative electrostatic potential enhances the inhibitory activity.

(Figure 5a) are found around the aromatic substituent attached to N4 as well as in the vicinity of N2. Moreover, an increase of the steric field in the region between N2 and S is detrimental for the inhibitory activity. The influence exerted by the nature of the heteroaromatic ring is reflected in the electrostatic contour shown in Figure 5b, which indicates that a negatively charged region around the ring is favorable for activity.

Because of the availability of X-ray crystallographic data for GSK-3, a mapping study was performed using the docking module of CMIP program.³¹ To validate this computational approach, we first explored the docking of three GSK3 inhibitors (I-5, indirubin-3'-monoxime, and alsterpauillone; Figure 6), whose binding mode has been determined by solving the X-ray structure of the complexes with GSK-3 β (PDB entries 1Q4L, 1Q4I, and 1Q3W).³² To avoid any bias toward the X-ray solution, CMIP calculations were performed by using the X-ray structure of the unbound enzyme (PDB entry 1I09). Present calculations, therefore, represent a stringent test because the side chains of certain residues (for instance, Arg141) exhibit notable differences between

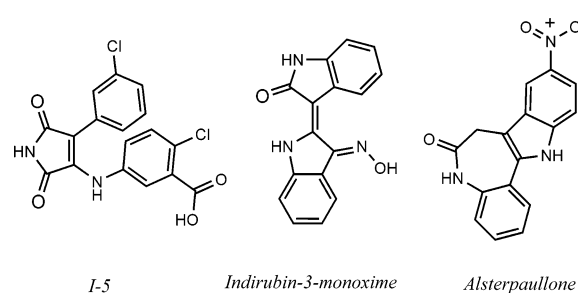


Figure 6. Chemical structures of I-5, indirubin-3-monoxime, and alsterpauillone

the X-ray structures determined for the enzyme bound to those inhibitors. For the three inhibitors, we identified the best poses out of first 10 possible solutions by comparing the positional root-mean square deviation (rmsd) between predicted and experimentally determined solutions (a RMSD threshold of ~ 2 Å is usually considered to be the upper limit for drug discovery).³³ For I-5, the best pose predicted correctly the experimental binding mode of the inhibitor with an rmsd of 1.3 Å. Two other poses close in energy to the best pose also reflected the alignment of the inhibitor with rmsds of 1.7 and 2.2 Å. Similar results were found for indirubin-3'-monoxime, where two poses reflected the experimentally determined solution with rmsds of 1.4 and 1.8 Å. Finally, six poses placed alsterpauillone at the same binding site detected in the X-ray structure, but with partial success, since the ligand was predicted to be rotated by $\sim 180^\circ$ along its main inertial axis, thus inverting the position of the pyrrole NH and amide C=O groups. This result can be mainly attributed to the absence of explicit water molecules in the enzyme structure used for docking, since binding of those groups is mediated by bridging water molecules. On the basis of these findings, though caution is required to determine accurately the binding mode of TDZDs, CMIP calculations appear suitable to identify potential binding sites in the enzyme.

The CMIP analysis was performed for TDZD compound 45 and allowed us to identify two potential binding sites. One of them is located in the vicinity of the activation loop, near residues Arg96, Arg180, and Lys205 (pocket on the right side of the enzyme as shown in Figure 5). There seems to be a nice shape complementarity between the binding pocket and the ligand, which adopts an eclipsed-like conformation with the two phenyl rings pointing toward the same face of the TDZD heteroaromatic ring. In this conformation cation- π interactions can be formed between the phenyl rings and the positively charged Arg92 and Arg96 residues. The binding of TDZDs to this pocket, which would explain the non-ATP competitive nature of these inhibitors (see above) might hinder the proper alignment of the substrate in the binding site, thus leading to inhibition of the phosphorylation mechanism. On the other hand, an alternative binding site is also found in the ATP-binding cavity (pocket on the left side of the enzyme as shown in Figure 7), where the ligand adopts an extended conformation. This recognition mode might not a priori justify the non-ATP competitive nature of TDZDs. However, based on the sensitivity of the GSK3 inhibitory data to the nature of the heteroaromatic ring and particularly the requirement of the sulfur atom in the

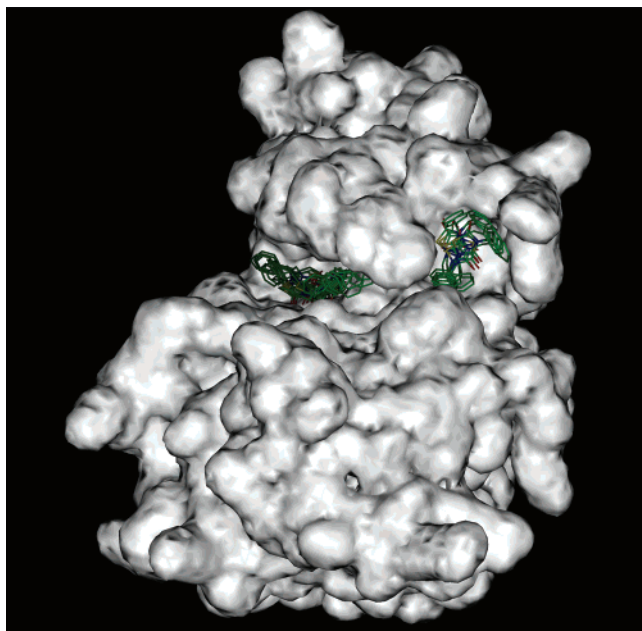


Figure 7. Preferred binding sites determined from CMIP mapping studies for TDZD inhibitor **45** onto the X-ray crystallographic structure of GSK3 (PDB entry 1I09).

TDZD scaffold for inhibitory activity, one might reinterpret the electrostatic requirement found in the CoMFA analysis in terms of the chemical susceptibility of TDZDs to react with the thiol group of Cys199, which lies close to the heteroaromatic ring of TDZD in some of the structures docked into the ATP-binding site. This finding would explain the apparent GSK3 specificity exhibited by TDZDs. During the revision of this manuscript, "selectivity filters" in the ATP-binding pocket of protein kinases discovered by bioinformatics techniques have been described.³⁴ One of them is a reactive cysteine residue within the active site. These data supports our preliminary conclusion.

Conclusion

Inspection of the results obtained for the different series of TDZD-related compounds examined here points out the important role played by the nature of the heteroaromatic ring in modulating the GSK3 inhibitory activity of these compounds. After an extensive SAR study among different heterocyclic families, TDZDs have been revealed as a privileged scaffold for the selective inhibition of GSK-3. Moreover, the SAR study also proves the influence played by aromatic substituents attached to the two nitrogen atoms of the TDZD ring. Mapping studies permit us to hypothesize two binding modes, which in turn might imply relevant differences in the mechanism that underly the inhibitory activity of TDZDs. Further studies, including directed mutagenesis and proteomic analysis, are in progress to clarify the mechanistic implications provided by these results. In the meantime, TDZDs have proved their *in vivo* activity, reducing the hyperphosphorylation of tau protein in a tet/GSK-3 double transgenic model,³⁵ being valuable candidates for drug development in the next future Alzheimer's therapy.

Experimental Section

Chemical Procedures. Melting points were determined with a Reichert-Jung Thermovar apparatus and are uncor-

rected. Flash column chromatography was carried out at medium pressure using silica gel (E. Merck, Grade 60, particle size 0.040–0.063 mm, 230–240 mesh ASTM) and preparative centrifugal circular thin-layer chromatography (CCTLC) on a circular plate coated with a 1 mm layer of Kieselgel 60 PF254, Merck, by using a Chromatotron with the indicated solvent as eluent. Compounds were detected with UV light (254 nm). ¹H NMR spectra were obtained on Varian XL-300 and Gemini-200 spectrometers working at 300 and 200 MHz, respectively. Typical spectral parameters: spectral width 10 ppm, pulse width 9 μs (57°), data size 32 K. ¹³C NMR experiments were carried out on the Varian Gemini-200 spectrometer operating at 50 MHz. The acquisition parameters: spectral width 16 kHz, acquisition time 0.99 s, pulse width 9 μs (57°), data size 32 K. Chemical shifts are reported in values (ppm) relative to internal Me₄Si and *J* values are reported in Hertz. Elemental analyses were performed by the analytical department at C. N. Q. O. (CSIC), and the results obtained were within ±0.4% of the theoretical values.

General Method for the Synthesis of *N*-Alkyl-maleimides. A 50 mL round bottom flask was charged with Ph₃P to which was added 25 mL of dry THF. The resulting clear solution was cooled to –70 °C, under nitrogen atmosphere. DIAD or DEAD depending of each case was added over 2–3 min. The yellow reaction mixture was stirred 5 min after which the corresponding alkyl alcohol was added over 1 min and stirred for 5 min. Then, maleimide was added to the reaction mixture as a solid. The resulting suspension was allowed to remain at –70 °C for 5 min during which time most of the maleimide dissolved. The cooling bath was then removed, and the reaction was stirred overnight at ambient temperature. The solvent was evaporated to dryness *in vacuo* and the residue purified by silica gel column chromatography using as eluent mixtures of solvents in the proportions indicated for each particulate case.

***N*-(Ethoxycarbonylmethyl)-maleimide (4).** Reagents: Ph₃P (1.31 g, 5 mmol), DEAD (0.8 mL, 5 mmol), ethyl glycolate (0.71 mL, 7.5 mmol), and maleimide (0.48 g, 5 mmol). Conditions: room temperature, overnight. Purification: silica gel column chromatography using AcOEt/hexane (1:3). Yield: 0.30 g (33%) as a colorless oil. ¹H NMR (CDCl₃): 1.25 (t, 3H, CH₂CO₂CH₂CH₃, *J* = 7.1 Hz); 4.20 (q, 2H, CH₂CO₂CH₂CH₃, *J* = 7.1 Hz); 4.24 (s, 2H, CH₂CO₂CH₂CH₃); 6.76 (d, 2H, CH=CH, *J* = 6.4 Hz). ¹³C NMR (CDCl₃): 13.7 (CH₂CO₂CH₂CH₃); 38.4 (CH₂CO₂CH₂CH₃); 61.5 (CH₂CO₂-CH₂CH₃); 134.3 (C=C); 166.9 (CO₂); 169.6 (C=O). Anal. (C₈H₉NO₄) C, H, N, S.

***N*-(*p*-Methoxy-benzyl)-maleimide (5).** Reagents: Ph₃P (1.31 g, 5 mmol), DEAD (0.8 mL, 5 mmol), *p*-methoxybenzyl alcohol (0.93 mL, 7.5 mmol), and maleimide (0.48 g, 5 mmol). Conditions: room temperature, overnight. Purification: silica gel column chromatography using AcOEt/hexane (1:3). Yield: 0.50 g (46%) as white solid; mp 99–102 °C. ¹H NMR (CDCl₃): 3.74 (s, 3H, OCH₃); 4.58 (s, 2H, CH₂Ph); 6.65 (d, 2H, CH=CH, *J* = 6.4 Hz); 6.8–7.2 (m, 4H, arom). ¹³C NMR (CDCl₃): 40.4 (CH₂Ph-OCH₃); 54.8 (OCH₃); 113.6; 128.2; 129.5; 158.8 (C arom); 133.8 (C=C); 170.1 (C=O). Anal. (C₁₂H₁₁NO₃) C, H, N, S.

***N*-Phenethyl-maleimide (6).** Reagents: Ph₃P (0.65 g, 2.5 mmol), DEAD (0.4 mL, 2.5 mmol), phenethyl alcohol (0.5 mL, 3.75 mmol), and maleimide (0.24 g, 2.5 mmol). Conditions: room temperature, overnight. Purification: silica gel column chromatography using AcOEt/hexane (1:4). Yield: 0.15 g (30%) as a white-yellow solid; mp 109–110 °C (lit.: 112 °C).²¹ ¹H NMR (CDCl₃): 2.90 (m, 2H, CH₂CH₂Ph); 3.77 (m, 2H, CH₂CH₂Ph); 6.66 (d, 2H, CH=CH, *J* = 6.4 Hz); 7.19–7.32 (m, 5H, arom). ¹³C NMR (CDCl₃): 34.5 (CH₂CH₂Ph); 38.9 (CH₂CH₂Ph); 126.6; 128.5; 128.7; 137.8 (C arom); 133.9 (C=C); 170.5 (C=O). Anal. (C₁₂H₁₁NO₂) C, H, N, S.

***N*-(*p*-Methoxy-phenethyl)-maleimide (7).** Reagents: Ph₃P (1.31 g, 5 mmol), DEAD (0.8 mL, 5 mmol), *p*-methoxyphenethyl alcohol (1.2 g, 7.5 mmol), and maleimide (0.48 g, 5 mmol). Conditions: room temperature, overnight. Purification: silica gel column chromatography using AcOEt/hexane (1:5). Yield: 0.71 g (60%) as a yellow solid; mp 79–81 °C. ¹H NMR (CDCl₃):

2.80 (m, 2H, CH₂CH₂Ph); 3.70 (m, 2H, CH₂CH₂Ph); 3.75 (s, 3H, OCH₃); 6.63 (d, 2H, CH=CH, *J* = 6.4 Hz); 6.8–7.1 (m, 4H, arom). ¹³C NMR (CDCl₃): 33.5 (CH₂CH₂Ph-OCH₃); 39.2 (CH₂CH₂Ph-OCH₃); 55.5 (OCH₃); 114.0; 129.7; 129.9; 158.4 (C arom); 133.9 (C=C); 170.5 (C=O). Anal. (C₁₃H₁₃NO₃) C, H, N, S.

N-(3-Phenyl-propyl)-maleimide (8). Reagents: Ph₃P (0.65 g, 2.5 mmol), DIAD (0.5 mL, 2.5 mmol), 3-phenyl-1-propanol (0.48 mL, 3.75 mmol), and maleimide (0.24 g, 2.5 mmol). Conditions: room temperature, overnight. Purification: silica gel column chromatography using AcOEt/hexane (1:4). Yield: 0.20 g (37%) as a white solid; mp 79–80 °C. ¹H NMR (CDCl₃): 1.92 (q, 2H, CH₂CH₂CH₂Ph, *J* = 7.1 Hz); 2.60 (t, 2H, CH₂CH₂CH₂Ph, *J* = 7.1 Hz); 3.55 (t, 2H, CH₂CH₂CH₂Ph, *J* = 7.1 Hz); 6.27 (d, 2H, CH=CH, *J* = 6.4 Hz); 7.12–7.28 (m, 5H, arom). ¹³C NMR (CDCl₃): 29.6 (CH₂CH₂CH₂Ph); 32.8 (CH₂CH₂CH₂Ph); 37.4 (CH₂CH₂CH₂Ph); 125.8; 128.1; 128.2; 140.7 (C arom); 133.7 (C=C); 170.6 (C=O). Anal. (C₁₃H₁₃NO₂) C, H, N, S.

N-(5-Phenyl-pentanyl)-maleimide (9). Reagents: Ph₃P (0.65 g, 2.5 mmol), DIAD (0.5 mL, 2.5 mmol), 5-phenyl-1-pentanol (0.63 mL, 3.75 mmol), and maleimide (0.24 g, 2.5 mmol). Conditions: room temperature, overnight. Purification: silica gel column chromatography using AcOEt/hexane (1:4). Yield: 0.32 g (52%) as white-yellow solid; mp 49–51 °C. ¹H NMR (CDCl₃): 1.20–1.38 (m, 2H, CH₂CH₂CH₂CH₂CH₂Ph); 1.52–2.02 (m, 4H, CH₂CH₂CH₂CH₂CH₂Ph); 2.57 (t, 2H, CH₂CH₂CH₂CH₂CH₂Ph, *J* = 7.3 Hz); 3.5 (t, 2H, CH₂CH₂CH₂CH₂CH₂Ph, *J* = 7.3 Hz); 6.65 (d, 2H, CH=CH, *J* = 6.4 Hz); 7.11–7.28 (m, 5H, arom). ¹³C NMR (CDCl₃): 25.9 (CH₂CH₂CH₂CH₂CH₂Ph); 28.0 (CH₂CH₂CH₂CH₂CH₂Ph); 30.6 (CH₂CH₂CH₂CH₂CH₂Ph); 35.4 (CH₂CH₂CH₂CH₂CH₂Ph); 37.3 (CH₂CH₂CH₂CH₂CH₂Ph); 125.4; 127.9; 128.0; 142.0 (C arom); 133.6 (C=C); 170.5 (C=O). Anal. (C₁₅H₁₇NO₂) C, H, N, S.

General Method for the Synthesis of Alkyl-rhodanines. Method A: To an equimolar solution of rhodanine with a base, 1 equiv of alkyl agent (alkyl halide) was added, with the conditions indicated for each particular case. The solvent was evaporated to dryness in vacuo and the residue purified by silica gel column chromatography using the appropriated eluent.

Method B: A 50 mL round-bottom flask was charged with Ph₃P to which was added 25 mL of dry THF. The resulting clear solution was cooled to –70 °C, under nitrogen atmosphere. DIAD or DEAD depending of each case was added over 2–3 min. The yellow reaction mixture was stirred 5 min after which the corresponding alkyl alcohol was added over 1 min and stirred for 5 min. Then, rhodanine was added to the reaction mixture as solid. The resulting suspension was allowed to remain at –70 °C for 5 min during, which time most of the rhodanine dissolved. The cooling bath was then removed, and the reaction was stirred overnight at ambient temperature. The solvent was evaporated to dryness in vacuo and the residue purified by silica gel column chromatography using as eluent mixtures of solvents in the proportions indicated for each particulate case.

N-Benzyl-rhodanine (22). Method B: Reagents: Ph₃P (1.31 g, 5 mmol), DIAD (1 mL, 5 mmol), benzyl alcohol (0.78 mL, 7.5 mmol), and rhodanine (0.67 g, 5 mmol). Conditions: 12 h at room temperature. Purification: silica gel column chromatography using AcOEt/hexane (1:4). Yield: 0.25 g (22%) as yellow solid, mp 84–85 °C (lit.: 85 °C).³⁶ ¹H NMR (CDCl₃): 3.9 (s, 2H); 5.2 (s, 2H, CH₂Ph); 7.3–7.4 (m, 5H, arom). ¹³C NMR (CDCl₃): 35.4 (CH₂); 47.6 (CH₂Ph); 128.2; 128.6; 129.1; 134.7 (C arom); 153.8 (C=O); 173.8 (C=S). Anal. (C₁₀H₉NS₂O) C, H, N, S.

N-Phenethyl-rhodanine (23). Method B: Reagents: Ph₃P (1.31 g, 5 mmol), DIAD (1 mL, 5 mmol), phenethyl alcohol (0.78 mL, 7.5 mmol), and rhodanine (0.67 g, 5 mmol). Conditions: Stirred at room temperature for 12 h. Purification: silica gel column chromatography using AcOEt/hexane (1:4). Yield: 0.55 g (42%) as yellow solid, mp 108–110 °C. ¹H NMR (CDCl₃): 2.9 (t, 2H, CH₂CH₂Ph, *J* = 8.1), 3.9 (s, 2H); 4.2 (s, 2H, CH₂CH₂Ph, *J* = 8.1); 7.4–7.9 (m, 5H, arom). ¹³C NMR (CDCl₃): 32.6

(CH₂CH₂Ph); 35.3 (CH₂); 45.7 (CH₂CH₂Ph); 126.8; 128.6; 128.6; 137.4 (C arom); 173.5 (C=O); 200.9 (C=S). Anal. (C₁₁H₁₁NS₂O) C, H, N, S.

N-Phenacyl-rhodanine (24). Method A: Reagents: Rhodanine (0.13 g, 1 mmol), K₂CO₃ (exceed), and acetophenone bromide (0.2 g, 1 mmol) in 25 mL of acetone. Conditions: Stirred at room temperature for 3 h. Isolation: The carbonate was filtered and the solvent evaporated to dryness in vacuo. Purification: preparative centrifugal circular thin-layer chromatography (CCTLC) using CH₂Cl₂. Yield: 0.04 g (15%) as brown oil. ¹H NMR (CDCl₃): 3.9 (s, 2H); 4.2 (s, 2H, CH₂COPh); 7.4–7.9 (m, 5H, arom). ¹³C NMR (CDCl₃): 37.6 (CH₂); 45.3 (CH₂COPh); 128.6; 128.7; 133.5; 135.3 (C arom); 170.5 (C=O); 194.1 (CH₂COPh); 197.6 (C=S). Anal. (C₁₁H₉NS₂O₂) C, H, N, S.

4-Benzyl-2,4-thiazolidine-3,5-dione (25). Method A: Reagents: 2,4-Thiazolidinedione (0.12 g, 1 mmol), sodium hydride (1 mmol, 0.04 g), and benzyl bromide (0.12 mL, 1 mmol) in 15 mL of DMF. Conditions: Stirred at room temperature for 8 h. Isolation: the solvent evaporated to dryness in vacuo. Purification: silica gel column chromatography using CH₂Cl₂. Yield: 0.14 g (66%) as white solid, mp 39–41 °C. ¹H NMR (CDCl₃): 3.8 (s, 2H, CH₂); 4.7 (s, 2H, CH₂Ph); 7.2–7.3 (m, 5H, arom); ¹³C NMR (CDCl₃): 33.6 (CH₂); 45.1 (CH₂Ph); 128.1; 128.5; 128.7; 134.9 (C arom); 171.0 (4-C=O); 171.5 (2-C=O). Anal. (C₁₀H₉NO₂S) C, H, N, S.

N-(*p*-Methoxy-benzyl)-rhodanine (26). Method B: Reagents: Ph₃P (0.65 g, 2.5 mmol), DEAD (0.4 mL, 2.5 mmol), *p*-methoxybenzyl alcohol (0.5 mL, 3.75 mmol), and rhodanine (0.33 g, 2.5 mmol). Conditions: room temperature, overnight. Purification: silica gel column chromatography using AcOEt/hexane (1:3). Yield: 0.15 g (32%) as a yellow oil; ¹H NMR (CDCl₃): 3.5 (s, 3H, CH₂Ph-*p*-OCH₃); 3.8 (s, 2H); 4.9 (s, 2H, CH₂Ph-*p*-OCH₃); 7.5–7.8 (m, 5H, arom). ¹³C NMR (CDCl₃): 37.5 (CH₂); 46.5 (CH₂Ph-*p*-OCH₃); 56.3 (CH₂Ph-*p*-OCH₃); 113.9; 126.5; 128.7; 159.8 (C arom); 171.2 (C=O); 197.6 (C=S). Anal. (C₁₀H₉NO₂S) C, H, N, S.

N-(*p*-Methoxy-phenethyl)-rhodanine (27). Method B: Reagents: Ph₃P (0.65 g, 2.5 mmol), DIAD (0.4 mL, 2.5 mmol), *p*-methoxyphenethyl alcohol (0.3 mL, 5 mmol), and rhodanine (0.33 g, 2.5 mmol). Conditions: room temperature, overnight. Purification: silica gel column chromatography using AcOEt/hexane (1:4). Yield: 0.22 g (33%), as a brown solid, mp 104–105 °C. ¹H NMR (CDCl₃): 2.8 (m, 2H, CH₂CH₂Ph); 3.7 (s, 3H, OCH₃); 3.9 (s, 2H, CH₂); 4.1 (s, 2H, CH₂CH₂Ph); 6.8–7.2 (m, 5H, arom, *J*₁ = 2.8, *J*₂ = 8.6). ¹³C NMR (CDCl₃): 31.5 (CH₂CH₂Ph); 35.1 (CH₂CH₂Ph); 45.6 (CH₂); 55.1 (OCH₃); 113.9; 129.2; 129.7; 158.9 (C arom); 173.4 (C=O); 200.8 (C=S). Anal. (C₁₂H₁₃NO₂S₂) C, H, N, S.

General Method for the Synthesis of Alkyl-dithiazolidinediones. To a solution of *N*-alkyl-formamide in dry toluene under nitrogen atmosphere, 2 equiv of chlorocarbonylsulfonyl chloride was slowly added. The resulting mixture was stirred at room temperature for 12 h. Then, the solvent was evaporated to dryness in vacuo and the residue purified by silica gel column chromatography using the appropriate eluent.

4-Methyl-1,2,4-dithiazolidine-3,5-dione (28). Reagents: *N*-Methyl-formamide (0.23 mL, 4 mmol) and chlorocarbonylsulfonyl chloride (0.676 mL, 8 mmol) in 20 mL of dry toluene. Conditions: Stirred at room temperature for 12 h. Purification: silica gel column chromatography using AcOEt/hexane (1:4) as eluent. Yield: 0.15 g (32%) as yellow solid, mp 37–38 °C (lit.: 38–39 °C).³⁷ ¹H NMR (CDCl₃): 3.2 (s, 3H, CH₃); ¹³C NMR (CDCl₃): 32.0 (CH₃); 167.1 (C=O). Anal. (C₃H₃NO₂S₂) C, H, N, S.

4-Phenyl-1,2,4-dithiazolidine-3,5-dione (29). Reagents: formamide (0.49 g, 4 mmol) and chlorocarbonylsulfonyl chloride (0.676 mL, 8 mmol) in 20 mL of dry toluene. Conditions: Stirred at room temperature for 12 h. Purification: silica gel column chromatography using AcOEt/hexane (1:1.5) as eluent. Yield: 0.15 g (17%) as a white-yellow solid; mp 165–167 °C (lit.: 168–169 °C).³⁷ ¹H NMR (CDCl₃): 7.14–7.5 (m, 5H, arom). ¹³C NMR (CDCl₃): 28.1 (2 CH₂); 42.3 (CH₂Ph);

127.5; 129.7; 129.9; 134.2 (C arom); 166.9 (2 C=O). Anal. (C₈H₅-NO₂S₂) C, H, N, S.

4-Benzyl-1,2,4-dithiazolidine-3,5-dione (30). Reagents: *N*-Benzylformamide (540 mg, 4 mmol) and chlorocarbonylsulfonyl chloride (0.676 mL, 8 mmol) in 20 mL of dry toluene. Conditions: Stirred at room temperature for 12 h. Purification: silica gel column chromatography using AcOEt/hexane (1:15) as eluent. Yield: 146 mg (17%), as a white solid. mp 90–92 °C (Lit.: 93–94 °C).³⁷ ¹H NMR (CDCl₃): 7.4–7.3 (m, 5H, arom); 4.9 (s, 2H, CH₂Ph). ¹³C NMR (CDCl₃): 49.3 (CH₂Ph); 133.9; 128.8; 128.6; 128.5 (C arom); 167.1 (C=O).

1,2-Dimethyl-4-Phenyl-1,2,4-triazolidine-3,5-dione (32). Reagents: 4-Phenylurazole (31) (0.09 g, 1 mmol), K₂CO₃ (excess), and iodomethane (0.14 g, 1 mmol) in 25 mL of acetone. Conditions: Refluxed for 6 h. Isolation: The carbonate was filtered and the solvent evaporated to dryness in vacuo. Purification: preparative centrifugal circular thin-layer chromatography (CCTLC) using CH₂Cl₂. Yield: 0.06 g (56%) as a white solid; mp 121–123 °C (lit.: 123–124 °C).³⁸ ¹H NMR (CDCl₃): 3.2 (s, 6H, 2 CH₃); 7.3–7.5 (m, 5H, arom). ¹³C NMR (CDCl₃): 32.3 (2 CH₃); 125.4; 128.0; 129.0; 131.5 (C arom); 153.5 (C=O). Anal. (C₁₀H₁₁N₃O₂) C, H, N, S.

1,2-Dibenzoyl-4-phenyl-1,2,4-triazolidine-3,5-dione (33). Reagents: 4-phenylurazole (31) (0.18 g, 1 mmol), sodium hydride (0.08 g, 2 mmol), and benzoyl chloride (0.18 mL, 1.5 mmol) in 15 mL of dimethylformamide (DMF). Conditions: Stirred at room temperature for 6 h. Purification: silica gel column chromatography using AcOEt/hexane (1:2) as eluent. Yield: 0.09 g (24%). mp 276–280 °C (Lit.: 272–273 °C).³⁸ ¹H NMR (CDCl₃): 7.4–7.5 (m, 5H, Ph); 7.5–8.1 (m, 10H, 2 × Bz). ¹³C NMR (CDCl₃): 126.0; 128.2; 130.9; 134.4 (C arom Ph); 129.5; 128.4; 130.2; 133.7 (C arom Bz); 164.5 (C=O); 172.3 (COPh). Anal. (C₂₂H₁₅N₃O₄) C, H, N, S.

1,2-Bis-(phenylcarboxymethyl)-4-phenyl-1,2,4-triazolidine-3,5-dione (34). Reagents: 4-phenylurazole (31) (0.35 g, 2 mmol), potassium hydroxide (0.11 g, 2 mmol), and acetophenone bromide (0.4 g, 2 mmol) in 15 mL of ethanol. Conditions: Refluxed for 10 h. Isolation: filtration of reaction mixture. Purification: recrystallization from EtOH/CH₂Cl₂. Yield: 0.24 g (28%), as a white solid. mp 208–210 °C (lit.: 205–206 °C).³⁸ ¹H NMR (CDCl₃): 5.0 (s, 4H, CH₂COPh); 7.4–7.9 (m, 15 H, arom). ¹³C NMR (CDCl₃): 53.0 (CH₂COPh); 126.0; 128.7; 128.4; 128.9; 129.2; 131.6; 134.1; 134.2 (C arom); 155.6 (C=O); 192.0 (COPh). Anal. (C₂₄H₂₀N₃O₄) C, H, N, S.

4-Benzyl-hydantoin (37). Reagents: Hydantoin (0.1 g, 1 mmol), sodium hydride (0.04 g, 1 mmol) and benzyl bromide (0.12 mL, 1 mmol) in 15 mL of DMF. Conditions: Stirred at room temperature for 12 h. Isolation: Evaporated to dryness in vacuo the solvent. Purification: silica gel column chromatography using AcOEt/hexane (1:1). Yield: 0.1 g (50%) as white solid; mp 138–139 °C. ¹H NMR (CDCl₃): 3.9 (s, 2H, CH₂); 4.6 (s, 2H, CH₂Ph); 5.4 (br, 1H, NH); 7.3–7.4 (m, 5H, arom). ¹³C NMR (CDCl₃): 42.0 (CH₂); 46.5 (CH₂Ph); 127.9; 128.3; 128.6; 135.8 (C arom.); 158.5 (2-C=O); 171.2 (4-C=O). Anal. (C₁₀H₁₀-N₂O₂) C, H, N

General Procedure for the Synthesis of 1,2,4-Thiadiazolidine-3,5-dione. Chlorine was bubbled slowly through a solution of aryl or alkyl isothiocyanate in dry hexane (25 mL), under nitrogen atmosphere, at –15 °C to –10 °C. Chlorine was generated by the addition of 35% HCl to KMnO₄. The temperature of the reaction mixture was carefully controlled during the addition step. At this point, the *N*-aryl- or *N*-alkyl-*S*-chlorisothiocarbonyl chloride was formed. Afterward, alkyl isocyanate was added, yielding, immediately, sparingly soluble 3-oxathiadiazolium salts. The mixture was stirred at room temperature between 8 and 10 h, producing the hydrolysis of these heterocyclic salts. After this time, the resulting product was purified by suction filtration and recrystallization or silica gel column chromatography using the appropriate eluent.

2-Ethyl-4-(4-nitrophenyl)-1,2,4-thiadiazolidine-3,5-dione (55). Reagents: 4-Nitrophenyl isothiocyanate (1.17 g, 6.5 mmol), 35% HCl (3.1 mL), KMnO₄ (0.5 g), and ethyl isocyanate (0.51 mL, 6.5 mmol) in THF. Conditions: room temperature,

10 h. Purification: silica gel column chromatography using AcOEt/hexane (1:4). Yield: 0.26 g (11%) as a yellow solid; mp 117–118 °C. ¹H NMR (CDCl₃): 1.34 (t, 3H, CH₂CH₃, *J* = 7.1 Hz); 3.77 (c, 2H, CH₂CH₃, *J* = 7.1 Hz); 7.6–8.4 (m, 5H, arom). ¹³C NMR (CDCl₃): 13.6 (CH₂CH₃); 40.3 (CH₂CH₃); 124.3; 127.6; 137.9; 147.1 (C arom.); 150.9 (3-C=O); 164.8 (5-C=O). Anal. (C₁₀H₉N₃SO₄) C, H, N, S.

2-Ethyl-4-phenyl-1,2,4-thiadiazolidine-3,5-dione (58). Reagents: Phenyl isothiocyanate (0.78 mL, 6.5 mmol), 35% HCl (3.1 mL), KMnO₄ (0.5 g), and ethyl isocyanate (0.51 mL, 6.5 mmol). Conditions: room temperature, 8 h. Isolation: filtration of reaction mixture. Purification: recrystallization from methanol. Yield: 0.43 g (30%) as a white solid; mp 174–179 °C. ¹H NMR (CDCl₃): 1.34 (t, 3H, CH₂CH₃, *J* = 7.2 Hz); 3.76 (c, 2H, CH₂CH₃, *J* = 7.2 Hz); 7.34–7.50 (m, 5H, arom.). ¹³C NMR (CDCl₃): 13.9 (CH₂CH₃); 40.3 (CH₂CH₃); 127.1; 129.0; 129.2; 132.6 (C arom.); 151.9 (3-C=O); 165.3 (5-C=O). Anal. (C₁₀H₁₀N₂SO₂) C, H, N, S.

4-(Ethoxycarbonylmethyl)-2-methyl-1,2,4-thiadiazolidine-3,5-dione (59). Reagents: Ethyl isothiocyanatoacetate (0.8 mL, 6.5 mmol), 35% HCl (3.1 mL), KMnO₄ (0.5 g), and methyl isocyanate (0.38 mL, 6.5 mmol). Conditions: room temperature, 8 h. Isolation: filtration of reaction mixture. Purification: recrystallization from hexane. Yield 0.28 g (20%) as white solid; mp 67–69 °C; ¹H NMR (CDCl₃): 1.3 (t, 3H, CH₂CO₂CH₂CH₃, *J* = 7.1 Hz); 3.2 (s, 3H, CH₃); 4.2 (c, 2H, CH₂CO₂CH₂CH₃, *J* = 7.1 Hz); 4.4 (s, 2H, CH₂CO₂CH₂CH₃); ¹³C NMR (CDCl₃): 14.0 (CH₂CO₂CH₂CH₃); 31.5 (CH₃); 42.7 (CH₂CO₂CH₂CH₃); 62.1 (CH₂CO₂CH₂CH₃); 152.6 (3-C=O); 166.4 (5-C=O); 166.4 (CO₂). Anal. (C₇H₁₀N₂SO₃) C, H, N, S.

Biological Procedures. GSK-3 Inhibition Assay. GSK-3 (rabbit GSK-3, Sigma) was incubated at 37 °C for a 20 min period in buffer [Tris pH = 7.5 (50 mM), EDTA (1 mM), EGTA (1 mM), and MgCl₂ (10 mM)] supplemented by the synthetic peptide GS-1 (15 μM final concentration) as substrate, ATP (15 μM), [³²P]ATP (0.2 μCi), and different concentrations of the product to be tested.³⁹ After that, aliquots of the reaction mixtures are added on phosphocellulose p81 papers. These papers are washed three times with phosphoric acid 1%, and the radioactivity incorporated in the GS-1 peptide is measured in a liquid scintillation counter. Dose–response profiles were generated, and the IC₅₀ value (concentration at which a 50% of enzyme inhibition is shown) for inhibition of GSK-3 by the test compound was calculated using a four-parameter logistic function.

Selectivity Panel Protein Kinase Assays. The pan-kinase screen was performed at CEREP (France). The members of the kinase selectivity panel were assessed as was described previously: Abl kinase assay,⁴⁰ CAM kinase assay,⁴¹ EGF-tyrosine kinase assay,⁴² IRK assay,⁴³ MAP kinase (ERK 42) assay,⁴⁴ MEK 1 kinase assay,⁴⁵ and protein kinase p56 assay.⁴⁶

The activated protein kinases were assayed for their ability to phosphorylate the appropriate peptide/protein substrate in the presence of 10 μM of test substance, respectively. Results are given as the mean of duplicate determinations for % inhibition compared to control incubations, in which the inhibitors were substituted with DMSO and reference compound (staurosporine).

CoMFA Analysis. The compounds were built from fragments in the Sybyl database. Each structure was initially fully optimized using the standard Tripos molecular mechanics force field using the default bond distances and angles as well as Gasteiger–Marsili charges.⁴⁷ Conformational analysis was carried out to define the low-energy conformations. The structures were fully geometrically optimized with the semi-empirical AM1 Hamiltonian⁴⁸ using MOPAC-6.0.⁴⁹ TDZD 43 was used as template molecule on which to align the other compounds using the minimum-energy conformation obtained as described above.

The CoMFA analysis is employed carried out using a grid spacing of 2.0 Å in the *x*, *y*, and *z* directions, and the grid region was automatically generated to encompass all molecules with an extension of 4.0 Å in each direction. A sp³ carbon and a

charge +1 were used as probes to generate the interaction energies at each lattice point. The default value of 30 kcal.mol⁻¹ was used as the maximum electrostatic and steric energy cutoff. Additionally, the molecular lipophilicity potential (MLP) was determined by using the method of Gaillard⁵⁰ to include hydrophobic effects into the CoMFA study. Partial least square (PLS) method was used to identify the relationship between the inhibitory activity data and the field potential values. Final non-cross-validated models were chosen on the basis of the best combinations of mentioned three fields.

All molecular modeling techniques and CoMFA studies described here were performed on Silicon Graphics workstation using the Sybyl 6.6 molecular modeling software from Tripos, Inc. St. Louis, MO.⁵¹

CMIP Calculations. Preferential binding sites of TDZDs on GSK3 protein surface were obtained using the docking module of the program CMIP.³¹ The protein (PDB entry 1I09) was mapped onto a 3D grid of the appropriate size with a 0.5 Å regular spacing (ca. 4000000 grid positions). Binding was assayed by exhaustive search of 8000 orientations (using nonredundant Euler angles) for every grid position. When necessary, flexible molecules were assayed as a family of standard rotamers. Docked positions were scored using interaction energies between the ligand and the protein, which were evaluated by adding electrostatic and van der Waals contributions (eq 1).

$$\Delta G_{\text{int}} = \Delta G_{\text{elect}} + \Delta G_{\text{vdw}} \quad (1)$$

The solvent-screened electrostatic interaction was determined by using the Mehler–Solmajer sigmoidal distance-dependent dielectric model,⁵² and the van der Waals component was evaluated by using a Lennard–Jones expression. Parameters for protein atoms were obtained from the amber98 force field.⁵³ For the ligand molecules, RESP atomic charges⁵⁴ determined at the HF/6-31G(d) level were used in conjunction with van der Waals parameters taken for related atoms in the amber98 force field.

Acknowledgment. The financial support from NeuroPharma is kindly acknowledged. Financial support from the Dirección General de Investigación Científica y Técnica (SAF2002-04282) is acknowledged.

Supporting Information Available: Plots of the best poses obtained from CMIP calculations for GSK-3 β inhibitors. This material is available free of charge via the Internet at <http://pubs.acs.org>.

References

- Wauwe, J. V.; Haefner, B. Glycogen synthase kinase-3 as drug target: From wallflower to center of attention. *Drug New Perspect.* **2003**, *16*, 557–565.
- Cohen, P.; Goedert, M. GSK-3 inhibitors: Development and therapeutic potential. *Nat. Rev. Drug Discovery* **2004**, *3*, 479–487.
- Kaidanovich, O.; Eldar-Finkelman, H. The role of glycogen synthase kinase-3 in insulin resistance and Type 2 diabetes. *Expert Opin. Ther. Targets* **2002**, *6*, 555–561.
- Grimes, C. A.; Jope, R. S. The multifaceted roles of glycogen synthase kinase 3 β in cellular signalling. *Prog. Neurobiol.* **2001**, *65*, 391–426.
- Hoeflich, K. P.; Luo, J.; Rubie, E. A.; Tsao, M. S.; Jin, O.; Woodgett, J. Role of glycogen synthase kinase-3 in TNF- α -induced NF- κ B activation and apoptosis in hepatocytes. *Nature* **2000**, *406*, 86–90.
- Martinez, A.; Castro, A.; Dorransoro, I.; Alonso, M. Glycogen Synthase Kinase 3 Inhibitors as new promising drugs for diabetes, neurodegeneration, cancer, and inflammation. *Med. Res. Chem.* **2002**, *22*, 373–384.
- Dorransoro, I.; Castro, A.; Martinez, A. Inhibitors of glycogen synthase kinase-3: Future therapy for unmet medical needs?. *Expert Opin. Ther. Pat.* **2002**, *12*, 1527–1536.
- Meijer, L.; Thunnissen, A. M.; White, A. W.; Garnier, M.; Nikolic, M.; Tsai, L. H.; Walter, J.; Cleverley, K. E.; Salinas, P. C.; Wu, Y. Z.; Biernat, J.; Mandelkow, E. M.; Kim, S. H.; Pettit, G. R. Inhibition of cyclin-dependent kinases, GSK-3 β and CK1 by hymenaldisine, a marine sponge constituent. *Chem. Biol.* **2000**, *7*, 51–63.20
- Leost, M.; Schultz, C.; Link, A.; Wu, Y. Z.; Biernat, J.; Mandelkow, E. M.; Bibb, J. A.; Snyder, G. L.; Greengard, P.; Zaharevitz, D. W.; Gussio, R.; Senderowicz, A. M.; Sausville, E. A.; Kunick, C.; Meijer, L. Paullones are potent inhibitors of glycogen synthase kinase-3 β and cyclin-dependent kinase 5/p25. *Eur. J. Biochem.* **2000**, *267*, 5983–5994.
- Leclerc, S.; Garnier, M.; Hoessel, R.; Marko, D.; Bibb, J. A.; Snyder, G. L.; Greengard, P.; Biernat, J.; Wu, Y. Z.; Mandelkow, E. M.; Eisenbrand, G.; Meijer, L. Indirubins inhibit glycogen synthase kinase-3 β and CDK5/p25, two protein kinases involved in abnormal tau phosphorylation in Alzheimer's disease. A property common to most cyclin-dependent kinase inhibitors. *J. Biol. Chem.* **2001**, *276*, 251–260.
- Smith, D. G.; Buffet, M.; Fenwick, A. E.; Haigh, D.; Ife, R. J.; Saunders, M.; Slingsby, B. P.; Stacey, R.; Ward, R. W. 3-Anilino-4-arylmaleimides: Potent and selective inhibitors of Glycogen synthase kinase-3 (GSK-3). *Bioorg. Med. Chem. Lett.* **2001**, *11*, 635–639.
- Martinez, A.; Alonso, M.; Castro, A.; Perez, C.; Moreno, F. J. First non-ATP competitive glycogen synthase kinase 3 β (GSK-3 β) inhibitors: thiadiazolidinones (TDZD) as potential drugs for the treatment of Alzheimer's disease. *J. Med. Chem.* **2002**, *45*, 1292–1299.
- Ter Haar, E.; Coll, J. T.; Austen, D. A.; Hsiao, H. M.; Swenson, L.; Jain, J. Structure of GSK-3 β reveals a primed phosphorylation mechanism. *Nat. Struct. Biol.* **2001**, *8*, 593–596.
- Dajani, R.; Fraser, E.; Roe, S. M.; Young, N.; Good, V.; Dale, T. C.; Pearl, L. H. Crystal Structure of Glycogen Synthase Kinase 3 β : Structural Basis for Phosphate-Primed Substrate Specificity and Autoinhibition. *Cell* **2001**, *105*, 721–732.
- Bertrand, J. A.; Thieffine, S.; Vulpetti, A.; Cristiani, C.; Valsolina, B.; Knapp, S.; Kalisz, H. M.; Flocco, M. Structural characterization of the GSK-3 active site using selective and nonselective ATP-mimetic inhibitors. *J. Mol. Biol.* **2003**, *33*, 393–407.
- Bhat, R.; Xue, Y.; Berg, S.; Hellberg, S.; Ormo, M.; Nilsson, Y.; Radesater, A. C.; Jerning, E.; Markgren, P. O.; Borgegard, T.; Nylof, M.; Gimenez-Cassina, A.; Hernandez, F.; Lucas, J. J.; Diaz-Nido, J.; Avila, J. Structural insights and biological effects of glycogen synthase kinase 3-specific inhibitor AR-A014418. *J. Biol. Chem.* **2003**, *278*, 45937–45945.
- Meijer, L.; Skaltsounis, A. L.; Magiatis, P.; Polychronopoulos, P.; Knockaert, M.; Leost, M.; Ryan, X. P.; Vonica, C. A.; Brivanlou, A.; Dajani, R.; Crovace, C.; Tarricone, C.; Musacchio, A.; Roe, S. M.; Pearl, L.; Greengard, P. GSK-3 selective inhibitors derived from Tyrian purple indirubins. *Chem. Biol.* **2003**, *10*, 1255–1266.
- Polychronopoulos, P.; Magiatis, P.; Skaltsounis, A.; Myrianthopoulos, V.; Mikros, E.; Tarricone, A.; Musacchio, A.; Roe, S. M.; Pearl, L.; Leost, M.; Greengard, P.; Meijer, L. Structural basis for the synthesis of indirubins as potent and selective inhibitors of glycogen synthase kinase-3 and cyclin-dependent kinases. *J. Med. Chem.* **2004**, *47*, 935–946.
- Alonso, M.; Martinez, A. GSK-3 inhibitors: discoveries and developments. *Curr. Med. Chem.* **2004**, *11*, 753–761.
- Cramer, R. D., III; Patterson, D. E.; Bunce, J. D. Comparative molecular field analysis (ComFA). 1. Effect of shape on binding of steroids to carrier proteins. *J. Am. Chem. Soc.* **1988**, *110*, 5959–5967.
- Walker, A. M. A high yielding synthesis of *N*-alkyl maleimides using a novel modification of the Mitsunobu reaction. *J. Org. Chem.* **1995**, *60*, 5352–5355.
- Zumach, G.; Weiss, W.; Kühle, E. Belgian Pat. 682820. Farbfabriken Bayer A. G., June 1966.
- MacLauchlin, C.; May, I. H.; Izydore, R. A. Synthesis and Cytotoxic action of 1-Oxoalkyl and 1,2-Dioxoalkyl-1,2,4-triazolidine-3,5-diones in Murine and Human tissue cultured Cells. *Arch. Pharm. Pharm. Med. Chem.* **1999**, *332*, 225–232.
- Hoshitsugu, A.; Matsui, M.; Fujii, A.; Kontani, T.; Koshiyuki, O.; Koizumi, T.; Shiro, M. Asymmetric Diels–Alder Reaction of optically active α -(2-exo-Hydroxy-O-bornyl)-sulfinylmaleimides and its application to optically active 5-functionalized Pyrrolines via Retro-Diels–Alder Reaction. *J. Chem. Soc., Perkin. Trans. I* **1994**, 25–39.
- Corrie, J. E. T. Thiol-reactive Fluorescent Probes for Protein Labelling. *J. Chem. Soc., Perkin. Trans. I* **1994**, 2975–2982.
- Janda, K. D.; Ashley, J. A.; Jones, T. M.; McLeod, D. A.; Schloeder, D. M.; Weinhaus, M. I. Immobilized Catalytic Antibodies in Aqueous and Organic Solvents. *J. Am. Chem. Soc.* **1990**, *112*, 8886–8888.
- Foye, W. O.; Tovovich, P. *N*-Glucopyranosyl-5-Aralkylidene-rhodanines: Synthesis and Antibacterial and Antiviral Activities. *J. Pharm. Sci.* **1977**, *66*, 1607–1611.
- Sudo, K.; Matsumoto, Y.; Matsushima, M.; Fujiwara, M.; Konno, K.; Shimotohno, K.; Shigetani, S.; Yokota, T. Novel Hepatitis C Virus Protease Inhibitors: Thiazolidine Derivatives. *Biochem. Biophys. Res. Commun.* **1997**, *238*, 643–647.

- (29) Mishra, S.; Srivastava, S. K.; Srivastava, S. D. Synthesis of 5-arylidene-2-aryl-3-(phenothiazino/benzo-triazoloacetamidyl)-1,3-thiazolidine-4-ones as antiinflammatory, anticonvulsant, analgesic and antimicrobial agents. *Indian. J. Chem. Sect. B.* **1997**, *36*, 826–830.
- (30) Peet, N. P. Genomics Research: Where are the drugs? *Idrugs* **2000**, *3*, 131–132.
- (31) Gelpi, J. L.; Kalko, S. G.; Barril, X.; Cirera, J., de la Cruz, X., Luque, F. J., Orozco, M. Classical molecular interaction potentials: improved setup procedure in molecular dynamics simulations of proteins. *Proteins* **2001**, *45*, 428–437.
- (32) Bertrand, J. A.; Thieffine, S.; Vulpetti, A.; Cristiani, C.; Valsasina, B.; Knapp, S.; Kalisz, H. M.; Flocco, M. Structural characterization of the GSK-3 β active site using selective and nonselective ATP-mimetic inhibitors. *J. Mol. Biol.* **2003**, *333*, 393–407.
- (33) Paul, N.; Rognan, D. ConsDock: A new program for the consensus analysis of protein–ligand interactions. *Proteins* **2002**, *47*, 521–533.
- (34) Cohen, M. S.; Zhang, C.; Shokat, K. M.; Taunton, J. Structural bioinformatics-based design of selective, irreversible kinase inhibitors. *Science* **2005**, *308*, 1318–1321.
- (35) Martín-Aparicio, E., Fuertes, A., Perez-Puerto, M. J., Perez, D., Alonso, M., Martínez, A., Medina, M. TDZDs: GSK-3 inhibitors as therapeutic agents for Alzheimer's disease and others tauopathies. *Neurobiol. Aging* **2004**, *25*, S596.
- (36) Girard, M. L.; Dreux, C. Possibilités Réactionnelles et Structurales de dérivés de la Thiazolidine. I-Addition, Substitution, Hydrolyse. *Bull. Soc. Chim. Fr.* **1968**, *3*, 3461–3468.
- (37) Zumach, G.; Weiss, W.; Kühle, E., British Patent 1,136,737 (June, 1966); *Chem. Abstr.* **1969**, *70*, 7795.
- (38) MacLauchlin, C.; May, I. H.; Izydore, R. A. Synthesis and cytotoxic action of 1-oxoalkyl and 1,2-dioxoalkyl-1,2,4-triazolidine-3,5-diones in murine and human tissue cultured cells. *Arch. Pharm. Pharm. Med. Chem.* **1999**, *332*, 225–232.
- (39) Woodget, J. R. Use of peptide substrates for affinity purification of protein-serine kinases. *Anal. Biochem.* **1989**, *180*, 237–241.
- (40) Parker, G. J.; Law, T. L.; Leno, F. J.; Bolger, R. E. Development of High Through-put screening assays using fluorescence polarization: nuclear receptor–ligand-binding and kinase/phosphatase assays. *J. Biomol. Screen.* **2000**, *5*, 77–88.
- (41) Lengyel I.; Nairn, A. C.; MC Cluskey, A.; Toth, B.; Penke, B.; Rostas, J. A. P. Auto-inhibition of Ca²⁺/calmodulin-dependent protein kinase II by its ATP-binding domain. *J. Neurochem.* **2001**, *76*, 1066–1072.
- (42) Carpenter, G.; King, L.; Cohen, S. Rapid enhancement of protein phosphorylation in A-431 cell membrane preparation by epidermal growth factor. *J. Biol. Chem.* **1979**, *254*, 4884–4891.
- (43) Al-Hasani, H.; Pablack, W.; Klein, H. W. Phosphoryl exchange is involved in the mechanism of the insulin receptor kinase. *FEBS Lett.* **1994**, *349*, 17–22.
- (44) Robbins, D. J.; Zhen, E.; Owaki, H. Regulation and properties of extracellular signal-regulated protein kinases 1 and 2 in vitro. *J. Biol. Chem.* **1993**, *268*, 5097–5106.
- (45) Williams, D. H.; Wilkinson, S. E.; Purton, T.; Lamont, A.; Flotow, A.; Murray, E. J. Ro 09-2210 exhibits potent anti-proliferative effects on activated T cells by selectively blocking MKK activity. *Biochemistry* **1998**, *37*, 9579–9585.
- (46) Cheng, H. C.; Nishio, H.; Hatase, O.; Ralph, S.; Wang, J. H. A synthetic peptide derived from p34cdc2 is a specific and efficient substrate of Src-family tyrosine kinases. *J. Biol. Chem.* **1992**, *13*, 9248–9256.
- (47) Gastaiger, J.; Marsili, M. Iterative partial equalization of orbital electronegativity-rapid access to atomic charges. *Tetrahedron* **1980**, *36*, 3219–3228.
- (48) Dewar, M. J. S.; Zoebisch, E. G.; Healy, E. F.; Stewart, J. J. AM1: a new general purpose quantum mechanical molecular model. *J. Am. Chem. Soc.* **1985**, *107*, 3902–3909.
- (49) Stewart, J. J. MOPAC: a semiempirical molecular orbital program. *J. Comput.-Aided Mol. Des.* **1990**, *4*, 1–105.
- (50) Gaillard, P., Carrupt, P. A.; Testa, B.; Boudon, A. Molecular lipophilicity potential, a tool in 3D QSAR: method and applications. *J. Comput.-Aided Mol. Des.* **1994**, *8*, 83–96.
- (51) SYBYL Molecular Modelling Package, version 6.6; Tripos St. Louis, MO.
- (52) Mehler, E. L.; Solmajer, T. Electrostatic effects in proteins: comparison of dielectric and charge models. *Protein Eng.* **1991**, *4*, 903–910.
- (53) Cornell, W. D.; Cieplak, P.; Bayly, C. I.; Gould, I. R.; Merz, K. M.; Ferguson, D. M.; Spellmeyer, D. C.; Fox, T.; Caldwell, J. W.; Kollman, P. A. A second generation force field for the simulation of proteins nucleic acids and organic molecules. *J. Am. Chem. Soc.* **1995**, *117*, 5179–5197.
- (54) Bayly, C. I.; Cieplak, P.; Cornell, W. D.; Kollman, P. A. A well-behaved electrostatic potential based method using charge restraints from deriving atomic charges: the RESP model. *J. Phys. Chem.* **1993**, *97*, 10268–10280.

JM040895G